Radiology

ORIGINAL RESEARCH • GENITOURINARY IMAGING

Comparison of Micro-US and Multiparametric MRI for Prostate Cancer Detection in Biopsy-Naive Men

Sangeet Ghai, MD • Nathan Perlis, MD, MSc • Chantal Atallah, MD • Sarah Jokhu, HBSc • Kateri Corr, BSc • Katherine Lajkosz, MSc • Peter F. Incze, MD • Alexandre R. Zlotta, MD, PhD • Umesh Jain, MD • Hannah Fleming, MD • Antonio Finelli, MD • Theodorus H. van der Kwast, MD, PhD • Masoom A. Haider, MD**

From the Joint Department of Medical Imaging, University Health Network–Sinai Health System–Women's, College Hospital, University of Toronto, Toronto General Hospital, 585 University Ave, 1PMB-292, Toronto, ON, Canada M5G 2N2 (S.G., H.F., M.A.H.); Division of Urology, Department of Surgical Oncology, University Health Network, University of Toronto, Toronto, Canada (N.P., S.J., K.C., K.L., A.R.Z., A.F.); Department of Pathology, Laboratory Medicine Program, University Health Network, University of Toronto, Toronto, Canada (C.A., T.H.v.d.K.); Department of Biostatistics, Princess Margaret Cancer Centre, University Health Network, University of Toronto, Toronto, Canada (K.L.); Department of Urology, Oakville Trafalgar Memorial Hospital, Toronto, Canada (P.F.I.); and Department of Surgery, University of Toronto, Toronto, Canada (U.J.). Received August 27, 2021; revision requested October 27; revision received April 19, 2022; accepted May 23. **Address correspondence to** S.G. (email: *Sangeet.Ghai@uhn.ca*).

Supported by the Innovation Fund of the Alternative Funding Plan for the Academic Health Sciences Centres of Ontario (project code MSU-19-003).

* T.H.v.d.K. and M.A.H. are co-senior authors.

Conflicts of interest are listed at the end of this article.

Radiology 2022; 000:1–10 • https://doi.org/10.1148/radiol.212163 • Content codes: GU MR US

Background: Multiparametric MRI has led to increased detection of clinically significant prostate cancer (csPCa). Micro-US is being investigated for csPCa detection.

Purpose: To compare multiparametric MRI and micro-US in detecting csPCa (grade group ≥2) and to determine the proportion of MRI nodules visible at micro-US for real-time targeted biopsy.

Materials and Methods: This prospective, single-center trial enrolled biopsy-naive men with suspected prostate cancer (PCa) between May 2019 and September 2020. All patients underwent multiparametric MRI followed by micro-US; findings at both were interpreted in a blinded fashion, followed by targeted biopsy and nontargeted systematic biopsy using micro-US. Proportions were compared using the exact McNemar test. The differences in proportions were calculated.

Results: Ninety-four men (median age, 61 years; IQR, 57–68 years) were included. MRI- and micro-US–targeted biopsy depicted csPCa in 37 (39%) and 33 (35%) of the 94 men, respectively ($P = .22$); clinically insignificant PCa in 14 (15%) and 15 (16%) ($P > .99$); and cribriform and/or intraductal PCa in 14 (15%) and 13 (14%) ($P > .99$). The MRI- plus micro-US–targeted biopsy pathway depicted csPCa in 38 of the 94 (40%) men. The addition of nontargeted systematic biopsy to MRI- plus micro-US–targeted biopsy did not enable identification of any additional men with csPCa but did help identify nine additional men with clinically insignificant PCa ($P = .04$). Biopsy was avoided in 32 of the 94 men (34%) with MRI and nine of the 94 men (10%) with micro-US ($P < .001$). Among 93 MRI targets, 62 (67%) were prospectively visible at micro-US.

Conclusion: MRI and micro-US showed similar rates of prostate cancer detection, but more biopsies were avoided with the MRI pathway than with micro-US, with no benefit of adding nontargeted systematic biopsy to the MRI- plus micro-US–targeted biopsy pathway. Most MRI lesions were prospectively visible at micro-US, allowing real-time targeted biopsy.

ClinicalTrials.gov registration no.: NCT03938376

Online supplemental material is available for this article.

During the past decade, multiparametric MRI (mpMRI) has made vast inroads in the diagnosis and staging of prostate cancer (PCa). Several level 1 evidence studies, including PRECISION (1), 4 M (2), MRI-FIRST (3), PRECISE (4), and PROMIS (5), have confirmed the superiority of MRI-targeted biopsy over transrectal US (TRUS)–guided systematic biopsies for the detection of clinically significant PCa (csPCa). Although mpMRI has improved detection rates, there are issues related to MRI cost, access, interpretation, and fusion biopsy expertise. In addition, although recommendations have been outlined for the minimal technical requirements and reporting of prostate mpMRI (6), studies have reported moderate interobserver agreement between readers (7,8) and variability in scan quality (9).

The value of hypoechoic areas at conventional TRUS in the prediction of PCa is poor, with a low positive predictive value of 18%–42% (10,11) and a low negative predictive value, missing csPCa in up to 48% of patients (12,13). This has resulted in conventional TRUS being used primarily for systematic biopsy guidance. In addition to missing smaller and atypically located cancers, nontargeted systematic biopsy sampling often helps detect indolent disease, leading to psychologic burden and overtreatment in some men.

More recently, micro-US has emerged as a promising imaging technology for PCa diagnosis (14). Micro-US

Abbreviations

Cr = cribriform, csPCa = clinically significant PCa, IDC = intraductal cancer, mpMRI = multiparametric MRI, PCa = prostate cancer, PI-RADS = Prostate Imaging Reporting and Data System, PRI-MUS = Prostate Risk Identification Using Micro-US, TRUS = transrectal US

Summary

Multiparametric MRI and micro-US showed similar prostate cancer detection rates in biopsy-naive men; although micro-US was inferior to multiparametric MRI for biopsy avoidance, most MRI lesions were visible at micro-US.

Key Results

- In a prospective study of 94 men with clinically suspected prostate cancer, micro-US– and multiparametric MRI-targeted biopsies enabled detection of clinically significant cancer (grade group 2 or higher) in 35% and 39% of men ($P = .22$) and cribriform and/or intraductal cancer in 14% and 15% of men, respectively ($P > .99$).
- The MRI pathway avoided biopsy in more men (34%) than did the micro-US pathway (10%) ($P < .001$).
- Sixty-seven percent of MRI lesions were visible at micro-US, allowing real-time targeted biopsy.

operates at frequencies of 29 MHz and allows for a fourfold higher crystal density along the transducer (512 vs 128 crystals). This provides a threefold improvement in spatial resolution, as low as 70 μm (the size of a prostatic duct), compared with conventional US (9–12 MHz) (15). However, similar to MRI, micro-US is also prone to interobserver variability in the interpretation of images.

Evidence from a large randomized clinical trial suggested that micro-US is more sensitive than conventional TRUS in the detection of PCa (16). During the trial, a five-point scoring system, Prostate Risk Identification Using Micro-US (PRI-MUS), was developed and validated to assess the risk of PCa for targeted biopsy with micro-US (17). On the basis of the above, our hypothesis was that micro-US would be noninferior to mpMRI in the detection of csPCa.

The primary objective of this prospective study was to compare mpMRI and micro-US in the detection of csPCa (grade group ≥2), the detection of clinically insignificant PCa (grade group 1), the proportion of men able to avoid biopsy with each modality, and the role of nontargeted systematic biopsy with use of micro-US with mpMRI. Secondary objectives included a comparison of cribriform (Cr) and/or intraductal cancer (IDC), hereafter Cr/IDC, detection and the proportion of MRI nodules visible at micro-US for real-time targeted biopsy.

Materials and Methods

This study (ClinicalTrials.gov: NCT03938376) was supported by the Innovation Fund of the Alternative Funding Plan for the Academic Health Sciences Centres of Ontario (project code MSU-19-003). The authors had full control of the data and the information submitted for publication.

Study Participants

The institutional review board at University Health Network, University of Toronto, approved this study, and participants provided informed consent. Between May 2019 and September 2020, consecutive men in whom PCa was clinically suspected because of a suspicious prostate-specific antigen level or abnormal digital rectal examination findings and no previous prostate biopsies were enrolled. Patients with any contraindication to mpMRI (ie, pacemaker, hip prosthesis leading to suboptimal diffusion-weighted image quality, severe claustrophobia, brain aneurysm clip, contraindication to MRI contrast media that prevented acquisition of dynamic contrast-enhanced series) were excluded.

MRI Protocol

All scans were obtained with a 3-T Siemens Magnetom Skyra Fit magnet without an endorectal coil. Sequences performed were as follows: T2-weighed imaging in all three planes, diffusion-weighted imaging (b values of 50, 900, 1600 sec/mm^2, with generation of apparent diffusion coefficient maps), and dynamic

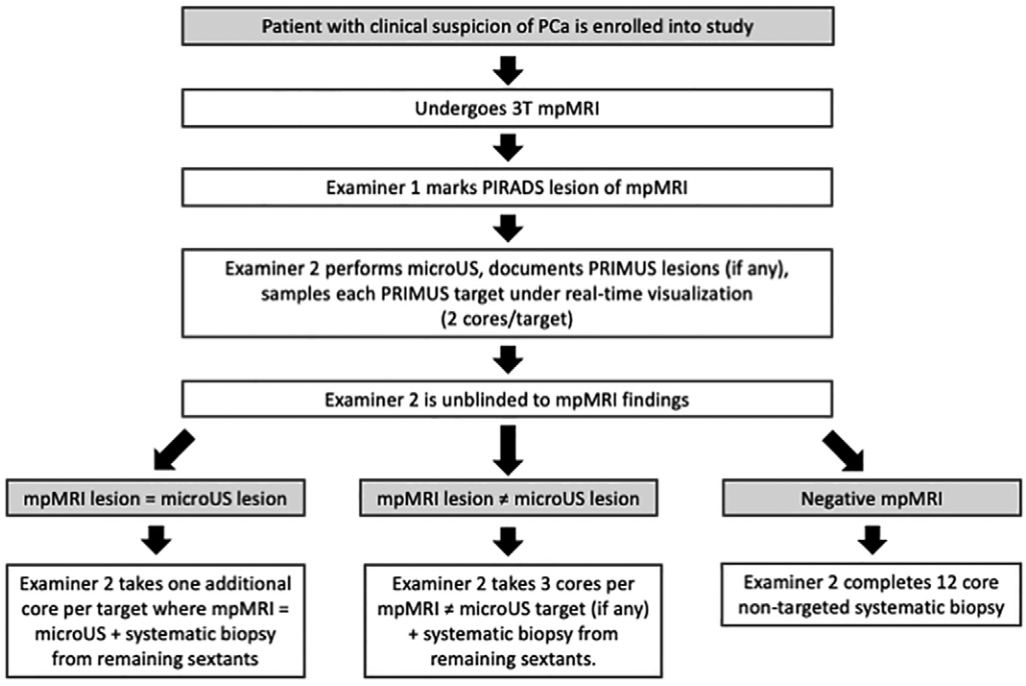

Figure 1: Flow diagram of the study design and biopsy workflow. mpMRI = multiparametric MRI, PCa = prostate cancer, PIRADS = Prostate Imaging Reporting and Data System, PRIMUS = Prostate Risk Identification Using Micro-US.

contrast-enhanced imaging (injection rate, 4 mL/sec). Detailed MRI acquisition parameters are outlined in Table E1 (online).

Workflow

All MRI scans were interpreted by one reader (M.A.H., with >15 years of experience in prostate MRI interpretation) using the Prostate Imaging Reporting and Data System (PI-RADS), version 2.1, reporting template. A PI-RADS score of 3 or greater and a maximum of four lesions per MRI examination (highest PI-RADS score) were reported. All micro-US examinations and biopsies were performed by one operator (S.G., with 5 years of experience) who had previously participated in the randomized controlled trial comparing micro-US to standard TRUS in the detection of PCa (16,17) and reviewed more than 400 images in the development of the PRI-MUS risk score (17) using micro-US. In addition, the micro-US operator had imaged more than 100 patients with the second-generation micro-US device before initiation of the study. Because a single reader had adequate expertise in micro-US operation at the institute, one experienced MRI reader interpreted all mpMRI scans to enable data comparability and reliability.

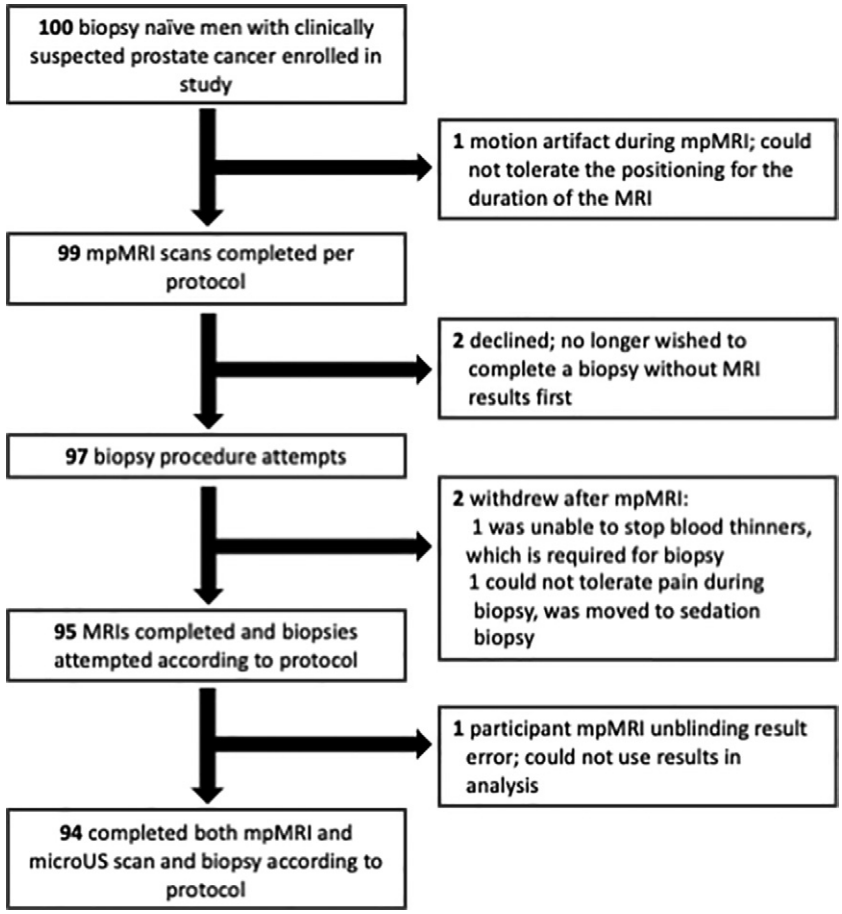

Figure 2: Flow diagram of men enrolled in study. mpMRI = multiparametric MRI.

Table 1: Participant and Clinical Details

Variable	All Participants (n = 94)	Participants with csPCa (n = 38)	Participants with Clinically Insignificant PCa or No Cancer (n = 56)	P Value
Age (y)				.004
Median	61 (57–68)	67 (58–70)	60 (56–64)	
Range	41–81	47–81	41–76	
PSA level (ng/mL)				.11
Median	6.37 (5.10–8.40)	6.31 (5.59–9.47)	6.40 (4.71–8.20)	
Range	1.80–13.9	4.50–13.9	1.80–12.00	
DRE status*				.001
Negative	57 (61)	14 (37)	43 (77)	
Positive	37 (39)	24 (63)	13 (23)	
Volume (cm^3)				<.001
Median	49 (34–64)	36 (28–51)	54 (43–75)	
Range	16–135	16–93	25–135	
Total no. of biopsy cores				
Median	15 (14–17)	16 (16–18)	15 (13–16)	<.001
Range	12–24	14–21	12–24	

Note.—Except where indicated, data in parentheses are the IQR. csPCa = clinically significant PCa, DRE = digital rectal examination, PCa = prostate cancer, PSA = prostate-specific antigen.

* Data are numbers of participants, with percentages in parentheses.

On the day of biopsy, transrectal micro-US scans were assessed, and up to four PRI-MUS targets were recorded. After the administration of local anesthesia, the operator sampled each of the PRI-MUS targets (two samples per PRI-MUS target) under real-time visualization. Thereafter, the micro-US operator was unblinded to the MRI findings and report by the study coordinators (S.J. and K.C.). In men with negative MRI findings (PI-RADS ≤2), completion nontargeted systematic biopsy sampling was performed as per the 12-core extended sextant template after micro-US assessment.

If the MRI finding was positive, with a PI-RADS score of 3 or greater, images with regions of interest were marked using Weasis software, version 3.0.4 (*https://nroduit.github.io/en*), and overlaid on the micro-US images using FusionVu software (Exact Imaging). For MRI lesions already sampled as PRI-MUS targets before unblinding, one additional sample was obtained from the site after unblinding, and the three samples were labeled concordant in micro-US and MRI. If an MRI site did not correspond with the previously sampled PRI-MUS targets, FusionVu was used for accurate targeting. Three cores were obtained for each of the MRI targets not visualized at micro-US and labeled as such. If the PRI-MUS targets sampled before unblinding were not identified at MRI, the containers (with two cores) were labeled micro-US targets only. Thereafter, nontargeted systematic biopsy samples were obtained from sextants not included in targeted sampling (Fig 1).

All pathology samples were reviewed by one specialist genitourinary pathologist (T.H.V.d.k., with >20 years of experience in interpreting prostate biopsy samples), along with a fellow (C.A., with 4 years of experience). The pathology slides were reviewed together in consensus. The final report was based on the interpretation of the specialist genitourinary pathologist.

Table 2: Comparison of Micro-US–targeted Biopsy, MRI-targeted Biopsy, and Nontargeted Systematic Biopsy for Cancer Detection at Participant Level

Variable	Micro-US–targeted Biopsy	MRI-targeted Biopsy	*P* Value
csPCa (grade group 2 or higher)	33 (35)	37 (39)	.22
Clinically insignificant PCa (grade group 1)	15 (17)	14 (16)	>.99
Cr/IDC	13 (14)	14 (15)	>.99
Negative*	9 (10)	32 (34)	<.001

Note.—Unless otherwise noted, values are numbers of participants (n = 94), with percentages in parentheses. Cr = cribriform, csPCa = clinically significant PCa, IDC =intraductal cancer, PCa = prostate cancer.

* Numbers in parentheses are the number of biopsies avoided.

Table 3: Comparison of Different Biopsy Pathways for Prostate Biopsy

Pathway	No. of Men with csPCa	No. of Men with Clinically Insignificant PCa	No. of Men with Cr/IDC PCa
MRI-targeted biopsy	37 (39)	14 (15)	14 (15)
Micro-US–targeted biopsy	33 (35)	15 (16)	13 (14)
Nontargeted systematic biopsy*	14 (15)	44 (47)	3 (3)
MRI-targeted biopsy plus micro-US–targeted biopsy	38 (40)	16 (17)	15 (16)
MRI-targeted biopsy plus micro-US–targeted biopsy plus nontargeted systematic biopsy	38 (40)	25 (27)	15 (16)

Note.—Unless otherwise noted values are numbers of men (n = 94), with percentages in parentheses. Cr = cribriform, csPCa = clinically significant PCa, IDC = intraductal cancer, PCa = prostate cancer.

* Nontargeted systematic biopsy is not a comprehensive systematic biopsy because sites of micro-US and multiparametric MRI targets were not included.

Statistical Analysis

Sample characteristics, stratified according to csPCa status, were summarized using descriptive statistics. Differences in continuous and categorical characteristics were assessed using the t test and Fisher exact test, respectively. The proportions of csPCa and clinically insignificant PCa detected were calculated for each pathway. The number of biopsies avoided was calculated by assuming that men with negative imaging results would avoid biopsy. The 95% CIs were calculated using the Clopper-Pearson method. Exact McNemar tests were used to compare the proportions of csPCa and clinically insignificant PCa detected with the mpMRI and micro-US pathways. The differences in the proportions of csPCa and clini-

Table 4: Comparison of Micro-US– and MRI-targeted Biopsies at Lesion Level

Modality	Total No. of Lesions Targeted for Biopsy	MRI Plus Micro-US Concordant Lesions	csPCa in Concordant Lesions	Discordant Lesions	csPCa in Discordant Lesions	*P* Value
MRI-targeted biopsy	93	62 (67)	36/62 (58)	31 (33)	8/31 (26)	.003
Micro-US–targeted biopsy	162	62 (38)	36/62 (58)	100 (62)	9/100 (9)	<.001

Note.—Except where indicated, data are numbers of targets, with percentages in parentheses. csPCa = clinically significant prostate cancer.

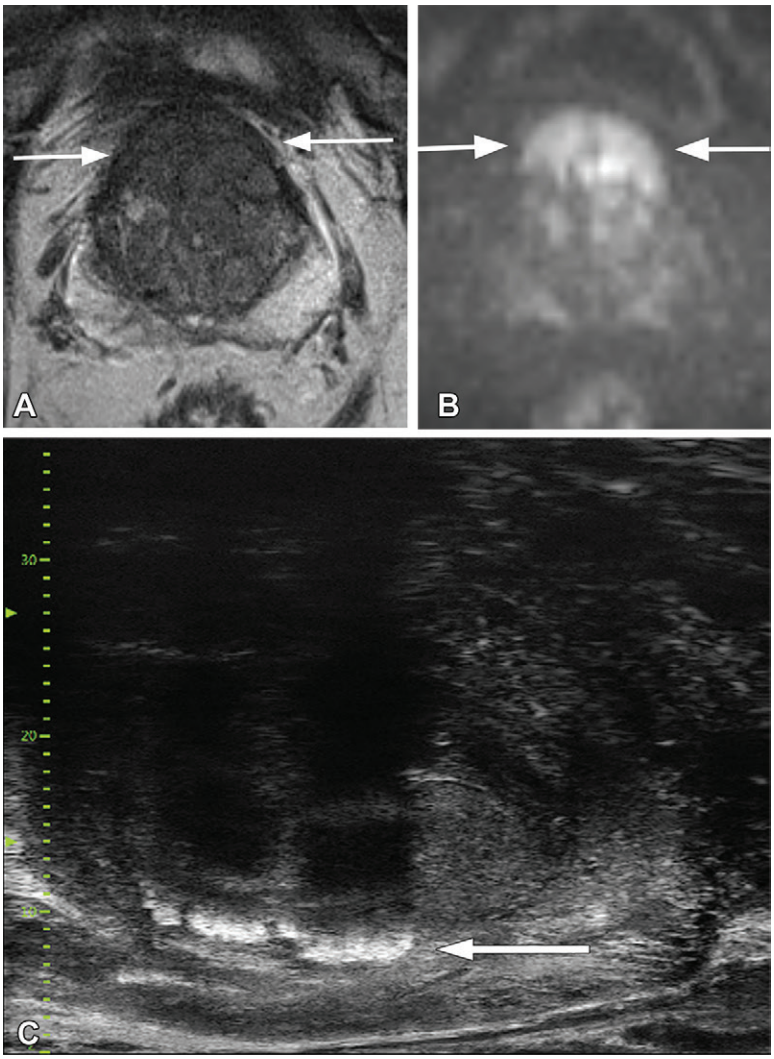

Figure 3: Images in a 71-year-old man with prostate-specific antigen level of 12.3 ng/mL. **(A)** T2-weighted and **(B)** diffusion-weighted MRI scans show a 2-cm Prostate Imaging Reporting and Data System, or PI-RADS, category 5 lesion (arrows) in the anterior transition zone. **(C)** Micro-US scan failed to depict the site of the tumor. Shadowing from calcification in corpora amylacea (arrow) further limits assessment of anterior gland in this man. Targeted biopsy revealed grade group 2 disease.

cally insignificant PCa detected were calculated, along with their 95% adjusted Wald CIs. All statistical analyses were conducted by an author (K.L., with 8 years of experience) using R software (version 4.1.0; R Foundation for Statistical Computing). All tests were two sided. $P < .05$ was considered to indicate a statistically significant difference.

Sample Size Calculation

Data from the PROMIS trial (5) suggested that mpMRI improved sensitivity over that with conventional TRUS from 0.48 to 0.93 with a test ratio of 0.52 (95% CI: 0.45, 0.60). To preserve at least half of this benefit, a test ratio of 0.8 (20%) was chosen as being equal to 50% of the effect from the upper bound of 0.6 to a ratio of unity (equal sensitivity). Assuming sensitivities of 0.75 and 0.66 for micro-US and mpMRI, 100 men would provide 80% power to reject the null hypothesis, assuming 80% agreement between modalities (α = 5%).

Results

Participant Characteristics

One hundred participants were enrolled in the study. Six men were excluded: two declined to undergo biopsy without having MRI results first; one could not stop taking his blood thinners as is required for biopsy; one was claustrophobic and was unable to complete the MRI examination; and one could not undergo biopsy because of rectal pain. The sixth participant was excluded because the biopsy operator was inadvertently unblinded to the MRI findings before biopsy. Therefore, 94 men were included for analysis (Fig 2). The median participant age was 61 years (IQR, 57–68 years). The median prostate-specific antigen level was 6.4 ng/mL (IQR, 5.1–8.4 ng/mL), and the median prostate volume was 48.5 cm^3 (IQR, 34.5–63.1 cm^3). Sixty-three of the 94 men (67%) had PCa and 38 of the 94 (40%) had csPCa (grade group 2 or greater) at biopsy. Clinical and participant details are provided in Table 1. The median time between mpMRI and micro-US biopsy was 7 days (IQR, 3–17 days).

Participant-level Analysis

Micro-US–targeted biopsy helped detect csPCa in 33 of the 94 men (35%; 95% CI: 26, 46), and mpMRI-targeted biopsy helped detect csPCa in 37 of 94 men (39%; 95% CI: 30, 50), resulting in a difference of −4% (95% CI: −10, 1; P = .22) and a relative detection rate of 0.89. Micro-US–targeted biopsy helped detect clinically insignificant PCa in 15 of the 94 men (16%; 95% CI: 9, 25), and the mpMRI pathway helped detect clinically insignificant PCa in 14 of the 94 men (15%; 95% CI: 8, 24), resulting in a difference of −1% (95% CI: −2, 4; $P > .99$) and a relative detection rate of 0.93. Nontargeted systematic biopsy helped detect clinically insignificant PCa sites in 44 men (91 samples). In 19 of these men, csPCa was identified at mpMRI or micro-US targets. The number of biopsies avoided was nine of 94 (10%; 95% CI: 5, 17) in the micro-US pathway and 32 of 94 (34%; 95% CI: 25, 45) in the mpMRI pathway, resulting in a difference of −24% (95% CI: −36, −12; $P < .001$) (Table 2). The mpMRI plus micro-US pathway helped detect csPCa in 38 of the 94 men, and no additional cases of csPCa were identified with the addition of nontargeted systematic biopsy. The mpMRI plus micro-US plus nontargeted systematic biopsy pathway helped detect clinically insignificant PCa in 25 of the 94 men (27%; 95% CI: 18, 37) compared with 15 of 94 (16%; 95% CI: 9, 25) in the micro-US pathway (P = .002) and 16 of 94 (17%; 95% CI: 10, 26) in the mpMRI plus micro-US pathway (P = .004) (Table 3).

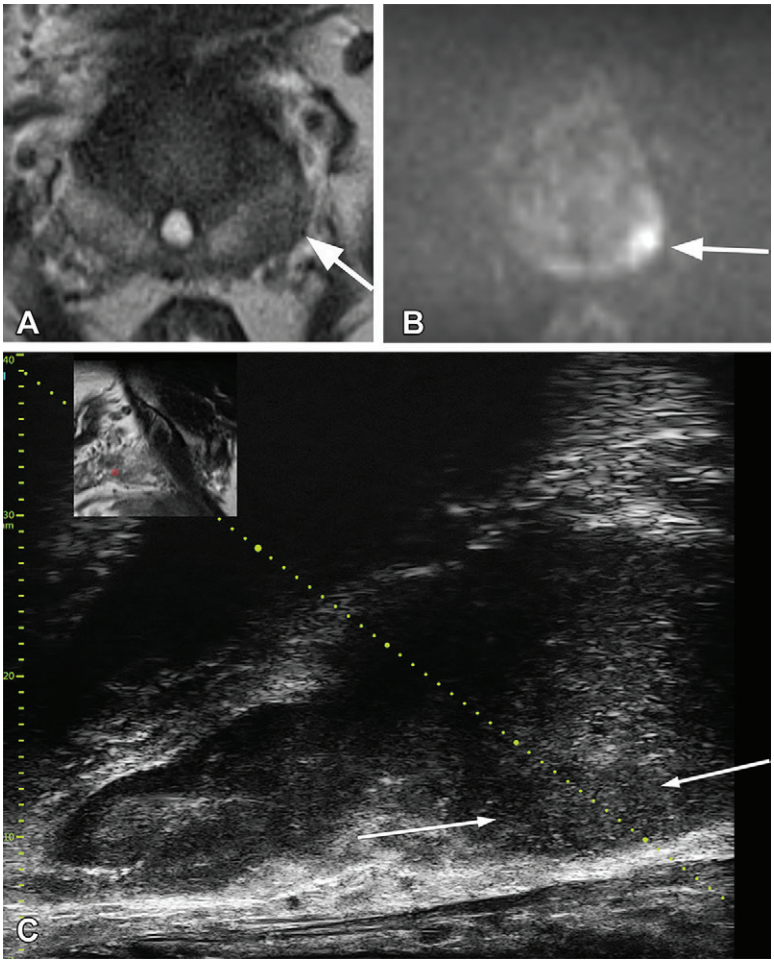

Figure 4: Images in a 52-year-old man with prostate-specific antigen level of 5.7 ng/mL. **(A)** T2-weighted and **(B)** high-*b*-value diffusion-weighted MRI scans show a Prostate Imaging Reporting and Data System, or PI-RADS, category 4 lesion (arrow) in the left base posterolateral peripheral zone. Micro-US did not prospectively depict the multiparametric MRI lesion. **(C)** Micro-US scan with FusionVu depicts the MRI lesion (arrows) in left lateral base retrospectively as a demarcated mildly hypoechoic nodule. Targeted biopsy revealed grade group 2 disease.

Lesion-level Analysis

Ninety-three lesions were identified at mpMRI in 62 men, and 162 lesions were identified at micro-US in 85 men. Of these, 62 lesions were concordant, identified with both modalities, and 36 of the 62 (58%) lesions were csPCa. Thirty-one discordant lesions were identified only with mpMRI, and 100 discordant lesions were identified only with micro-US. Forty-four of the 93 (46%) MRI lesions were positive for csPCa in 37 men at targeted biopsy, and 45 of the 162 (27%) micro-US lesions were positive for csPCa in 33 men at targeted biopsy (eight csPCa lesions were identified only with mpMRI and a further nine lesions were identified only with micro-US). For micro-US, 117 targets in 91 men were not csPCa (mean, 1.3 per participant), whereas 49 mpMRI targets in 62 men did not reveal csPCa (mean, 0.8 per participant). Of the eight csPCa lesions identified only at mpMRI, micro-US did not depict csPCa in five participants but depicted an additional site of csPCa in three participants. Nine csPCa lesions were identified only at micro-US: Two sites were in one participant for whom mpMRI did not depict any csPCa, whereas mpMRI depicted csPCa at a different location in seven men. Lesions visualized with both modalities were significantly more likely to be csPCa than lesions identified with one modality (Table 4). Thirty-seven of 898 nontargeted systematic biopsy cores in 14 men were positive for csPCa; 33 of these sites were adjacent to csPCa detected with mpMRI- or micro-US–targeted biopsy. Of the 44 mpMRI lesions with csPCa, eight were in the transition zone; two of these eight lesions were identified prospectively at micro-US. For micro-US, two of 45 true-positive lesions were in the transition zone.

Cr/IDC Histologic Findings

Cr/IDC PCa was identified in 15 men, and 12 of 15 were identified at concordant MRI and micro-US target sites. Cr/IDC PCa was identified only at MRI-targeted biopsy in two men and at micro-US–targeted biopsy in another man ($P > .99$). Nontargeted systematic biopsy did not identify any additional men with Cr/IDC PCa, although it detected Cr/IDC PCa in three of 898 samples in three men (Tables 2, 3).

Discussion

Prospective blinded studies comparing micro-US and multiparametric MRI (mpMRI) are lacking in the literature (18–24). Our prospective study compared the two modalities in a blinded fashion in a homogeneous biopsy-naive sample using mpMRI acquisition and reporting as per minimal requirements outlined in the Prostate Imaging Reporting and Data System document. Micro-US–targeted biopsy and mpMRI-targeted biopsy had comparable detection rates for clinically significant prostate cancer (csPCa) (35% vs 39%, $P = .22$), clinically insignificant prostate cancer (17% vs 16%, $P > .99$), and cribriform and/or intraductal histologic features (14% vs 15%, $P > .99$). However, the micro-US–only pathway was inferior to the MRI-only pathway in biopsy avoidance (10% vs 34%, $P < .001$). In addition, the mpMRI-targeted biopsy plus micro-US–targeted biopsy pathway without additional nontargeted systematic biopsy decreased the detection of clinically insignificant PCa without any tradeoff in csPCa detection. Furthermore, 62 of 93 (67%) mpMRI targets were prospectively visible at micro-US, enabling accurate targeted biopsy.

The prevalence of csPCa in our study (40%) was similar to that in contemporary sample groups (1,4). Three of five csPCas missed at micro-US were in the anterior transition zone (Fig 3). The PRI-MUS protocol (17) focuses on identifying suspicious areas at micro-US in the peripheral zone and does not include transition zone assessment. The benefit of the present micro-US platform over conventional TRUS is lost at a greater depth from the rectum, particularly in larger

glands. In addition, shadowing from calcification in the corpora amylacea can limit assessment of the anterior gland. These factors may have led to transition zone lesions going undetected at micro-US. csPCa in the peripheral zone was missed with micro-US in two men; in one of these men, the csPCa was retrospectively identified by the operator as a hypoechoic lesion (Fig 4).

One man in whom mpMRI failed to depict the site of csPCa was noted to have a "smudgy pattern" PRI-MUS 4 hypoechoic lesion at micro-US in the peripheral zone (Fig 5). Nonvisualization of csPCa at mpMRI has been attributed to a "sparse" tumor intermixed with normal tissue, which may then not be identified at diffusion-weighted imaging (25). Ductal pattern loss in a focal area of the gland or marked hypoechogenicity (Fig 6), other than those described in the PRI-MUS protocol, are in our experience helpful micro-US features in identifying cancer. Because micro-US relies on high-resolution morphologic assessment to detect csPCa, it may be able to help detect PCa not identified at mpMRI. Similar to our study, Lughezzani et al (18) reported a 2.6% improvement in csPCa detection by adding micro-US targets to MRI targets and systematic biopsy.

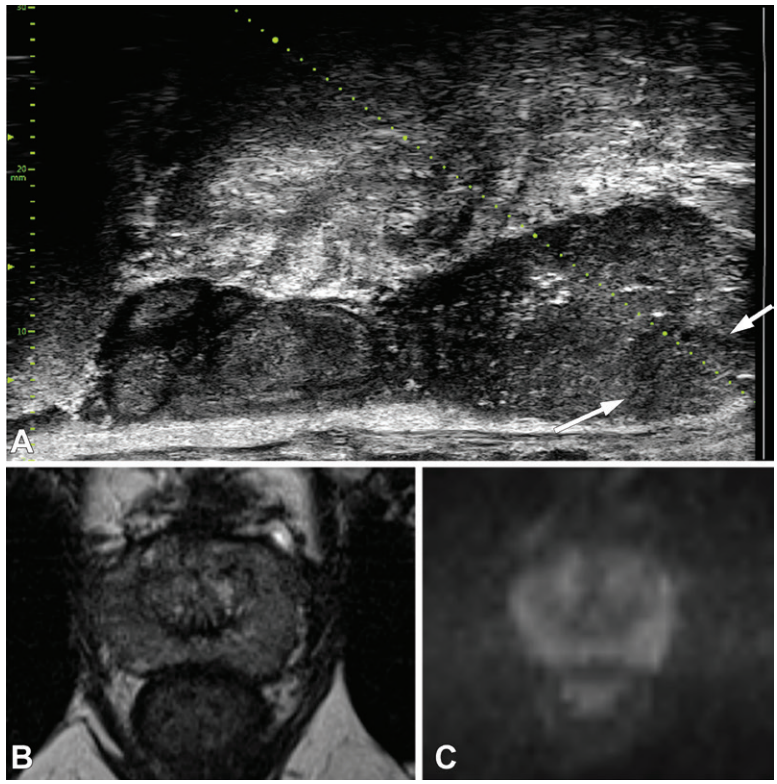

Figure 5: Images in a 49-year-old man with prostate-specific antigen level of 8.26 ng/mL. **(A)** A Prostate Risk Identification Using a Micro-US category 4 nodule (arrows) was identified in the left mid gland peripheral zone. The lesion was not identified at multiparametric MRI. **(B, C)** Corresponding T2-weighted (**B**) and high-*b*-value diffusion-weighted (**C**) MRI scans are shown. Targeted biopsy revealed grade group 2 disease.

Micro-US uses morphologic assessment of the gland similar to that with T2-weighted MRI, but at a higher resolution. Although the recommended in-plane resolution for T2-weighted imaging is less than 0.7-mm phase × less than 0.4-mm frequency direction, micro-US provides a resolution of up to 0.07 × 0.07 mm in the axial plane. However, micro-US lacks the functional assessment component of MRI (diffusion-weighted imaging and dynamic contrast-enhanced sequences) for the interrogation of suspicious sites based on morphologic features. This may be the primary reason for the higher number of false-positive lesions identified at micro-US than at mpMRI in our study. Similarly, Lughezzani et al (18) reported a relative specificity for micro-US of 29%, whereas Wiemer et al (21) reported a 15% specificity in their study.

Cr/IDC are histologic features associated with adverse clinical outcomes. Although the visibility of Cr/IDC PCa at MRI is still debated (26–28), our prospective study provides evidence that it can be identified at MRI and, for the first time, assessed its visibility at micro-US. MRI- and micro-US–targeted biopsy reassuringly depicted Cr/IDC PCa in 93% and 87% of men, respectively, whereas nontargeted systematic biopsy did not identify any additional man with Cr/IDC PCa in our study.

The addition of nontargeted systematic biopsy to MRI- and micro-US–targeted biopsy did not enable the identification of any additional men with csPCa but led to a significant increase in the detection of clinically insignificant PCa (nine additional men, $P = .004$). Although the addition of nontargeted systematic biopsy to MRI-targeted biopsy has been shown to increase the detection of both csPCa and clinically insignificant PCa (29,30), our study shows that the replacement of nontargeted systematic biopsy with micro-US–targeted biopsy may be a better alternative. A total of 898 nontargeted systematic biopsy cores could have been avoided in 94 men, with a 36% (nine of 25) decrease in the detection of clinically insignificant PCa.

Ukimura et al (31) showed that visibility of lesions at TRUS facilitates targeted biopsies. In our study, 67% of the mpMRI lesions (62 of 93) were prospectively visible at micro-US. In comparison, van de Ven et al (32) reported that with previous knowledge of MRI, 24 of 56 (43%) MRI lesions were visible at conventional TRUS during fusion biopsy ($P = .04$). Once the lesions were visible during biopsy, the incidence of csPCa in targeted biopsy was similar whether micro-US (36 of 62 [58%]) or conventional TRUS with fusion biopsy (14 of 24 [58%]) was used ($P = .98$). This highlights the advantage of micro-US for targeted biopsy over MRI fusion–targeted biopsy coupled with conventional TRUS (6–9 MHz). Similarly, Cornud et al (33) reported that 90% of MRI lesions (114 of 127) were visible at micro-US with previous knowledge of MRI findings; 61% (70 of 114) of the lesions were csPCa at targeted biopsy.

Our study has several limitations. First, an ideal reference standard, such as transperineal template mapping biopsy, was not used, which may have led to some cancers going

undetected. Second, to reduce the number of cores taken, systematic biopsy samples were not obtained from areas of micro-US– or mpMRI-targeted biopsy. Therefore, we cannot compare with standard systematic biopsy and instead refer only to nontargeted systematic biopsy. Third, two cores were obtained for lesions identified solely at micro-US, whereas three cores were obtained for MRI and concordant targets. It is possible that this may have adversely affected csPCa detection for micro-US–only lesions. Fourth, FusionVu technology was used to target lesions identified at mpMRI only. FusionVu is a recent addition to micro-US and has not been validated independently to assess its accuracy in targeting. Finally, single operators interpreted mpMRI and micro-US images. However, studies have reported a short learning curve for the interpretation of micro-US images (17,21).

In conclusion, our results show that micro-US is an attractive addition to multiparametric MRI in the detection of clinically significant prostate cancer and that both modalities complement each other. Multicenter randomized trials comparing the two techniques are required to corroborate our findings and establish micro-US in the diagnostic pathway for cancer detection.

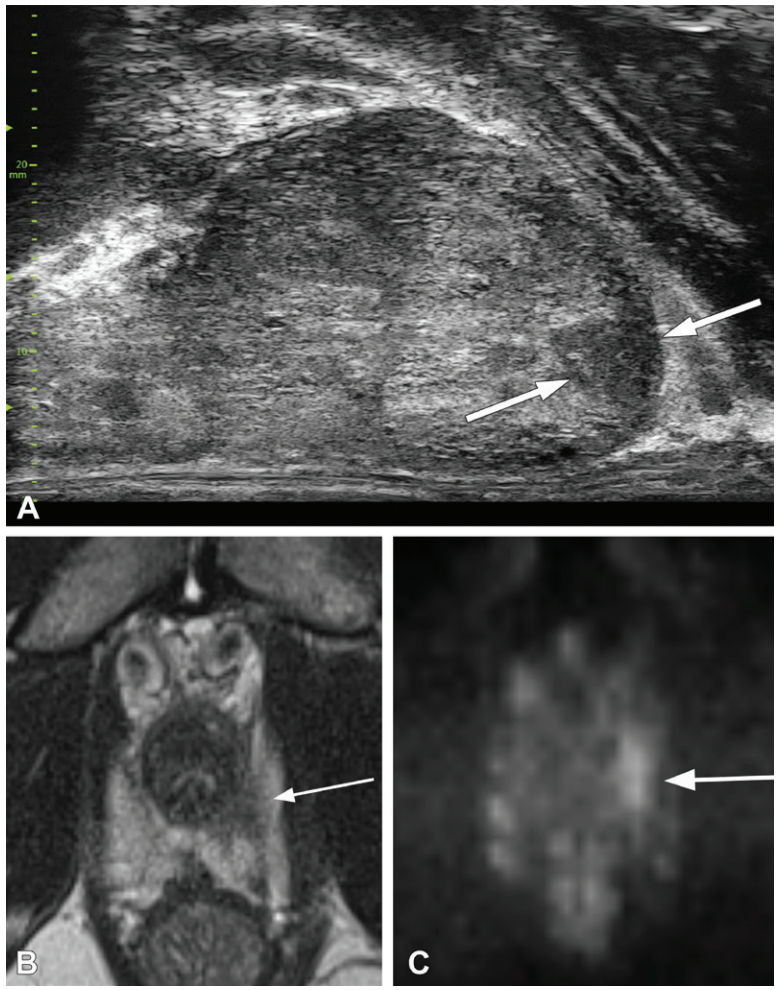

Figure 6: Images in a 60-year-old man with prostate-specific antigen level of 4.5 ng/mL. **(A)** Micro-US scan shows a 6-mm hypoechoic lesion (arrows) in the left medial apex. **(B, C)** Multiparametric MRI scans (axial T2-weighted image [**B**] and diffusion-weighted image [**C**]) show corresponding Prostate Imaging Reporting and Data System, or PI-RADS, category 4 lesion (arrow). Targeted biopsy revealed grade group 2 disease.

Author contributions: Guarantors of integrity of entire study, **S.G., H.F., A.F.**; study concepts/study design or data acquisition or data analysis/interpretation, all authors; manuscript drafting or manuscript revision for important intellectual content, all authors; approval of final version of submitted manuscript, all authors; agrees to ensure any questions related to the work are appropriately resolved, all authors; literature research, **S.G., N.P., H.F.**; clinical studies, **S.G., N.P., S.J., K.C., P.F.I., U.J., T.H.v.d.K.**; experimental studies, **N.P., C.A.**; statistical analysis, **K.C., K.L.**; and manuscript editing, **S.G., N.P., C.A., K.L., A.R.Z., H.F., A.F., T.H.v.d.K., M.A.H.**

Data sharing: Data generated or analyzed during the study are available from the corresponding author by request.

Disclosures of conflicts of interest: **S.G.** Grant from Exact Imaging for micro-US guided Focal Laser Ablation for Prostate Cancer feasibility study. **N.P.** No relevant relationships. **C.A.** No relevant relationships. **S.J.** No relevant relationships. **K.C.** No relevant relationships. **K.L.** No relevant relationships. **P.F.I.** No relevant relationships. **A.R.Z.** No relevant relationships. **U.J.** Honorarium for speaker from Astellas and Tersera. **H.F.** Participation on a data safety monitoring board or advisory board for University Health Network. **A.F.** Participation on a data safety monitoring board or advisory board for Princess Margaret Cancer Center-University Health Network. **T.H.v.d.K.** No relevant relationships. **M.A.H.** No relevant relationships.

References

1. Kasivisvanathan V, Rannikko AS, Borghi M, et al. MRI-targeted or standard biopsy for prostate-cancer diagnosis. N Engl J Med 2018;378(19):1767–1777.
2. van der Leest M, Cornel E, Israël B, et al. Head-to-head comparison of transrectal ultrasound-guided prostate biopsy versus multiparametric prostate resonance imaging with subsequent magnetic resonance-guided biopsy in biopsy-naïve men with elevated prostate-specific antigen: a large prospective multicenter clinical study. Eur Urol 2019;75(4):570–578.
3. Rouvière O, Puech P, Renard-Penna R, et al. Use of prostate systematic and targeted biopsy on the basis of multiparametric MRI in biopsy-naive patients (MRI-FIRST): a prospective, multicentre, paired diagnostic study. Lancet Oncol 2019;20(1):100–109.
4. Klotz L, Chin J, Black PC, et al. Comparison of multiparametric magnetic resonance imaging-targeted biopsy with systematic transrectal ultrasonography biopsy for biopsy-naive men at risk for prostate cancer: a phase 3 randomized clinical trial. JAMA Oncol 2021;7(4):534–542.
5. Ahmed HU, El-Shater Bosaily A, Brown LC, et al. Diagnostic accuracy of multi-parametric MRI and TRUS biopsy in prostate cancer (PROMIS): a paired validating confirmatory study. Lancet 2017;389(10071):815–822.
6. Turkbey B, Rosenkrantz AB, Haider MA, et al. Prostate Imaging Reporting and Data System Version 2.1: 2019 update of Prostate Imaging Reporting and Data System Version 2. Eur Urol 2019;76(3):340–351.
7. Girometti R, Giannarini G, Greco F, et al. Interreader agreement of PI-RADS v. 2 in assessing prostate cancer with multiparametric MRI: A study using whole-mount histology as the standard of reference. J Magn Reson Imaging 2019;49(2):546–555.
8. Greer MD, Shih JH, Lay N, et al. Interreader Variability of Prostate Imaging Reporting and Data System Version 2 in detecting and assessing prostate cancer lesions at prostate MRI. AJR Am J Roentgenol 2019;212(6):1197–1205.
9. Giganti F, Allen C. Imaging quality and prostate MR: it is time to improve. Br J Radiol 2021;94(1118):20200934.
10. Flanigan RC, Catalona WJ, Richie JP, et al. Accuracy of digital rectal examination and transrectal ultrasonography in localizing prostate cancer. J Urol 1994;152(5 Pt 1):1506–1509.

11. Loch T, Eppelmann U, Lehmann J, Wullich B, Loch A, Stöckle M. Transrectal ultrasound guided biopsy of the prostate: random sextant versus biopsies of sono-morphologically suspicious lesions. World J Urol 2004;22(5):357–360.
12. Carter HB, Hamper UM, Sheth S, Sanders RC, Epstein JI, Walsh PC. Evaluation of transrectal ultrasound in the early detection of prostate cancer. J Urol 1989;142(4):1008–1010.
13. Ghai S, Toi A. Role of transrectal ultrasonography in prostate cancer. Radiol Clin North Am 2012;50(6):1061–1073.
14. Pavlovich CP, Cornish TC, Mullins JK, et al. High-resolution transrectal ultrasound: pilot study of a novel technique for imaging clinically localized prostate cancer. Urol Oncol 2014;32(1):34.e27–34.e32.
15. Laurence Klotz CM. Can high resolution micro-ultrasound replace MRI in the diagnosis of prostate cancer? Eur Urol Focus 2020;6(2):419–423.
16. Pavlovich CP, Hyndman ME, Eure G, et al. A multi-institutional randomized controlled trial comparing first-generation transrectal high-resolution micro-ultrasound with conventional frequency transrectal ultrasound for prostate biopsy. BJUI Compass 2020;2(2):126–133.
17. Ghai S, Eure G, Fradet V, et al. Assessing cancer risk on novel 29 mhz micro-ultrasound images of the prostate: creation of the micro-ultrasound protocol for prostate risk identification. J Urol 2016;196(2):562–569.
18. Lughezzani G, Saita A, Lazzeri M, et al. Comparison of the diagnostic accuracy of micro-ultrasound and magnetic resonance imaging/ultrasound fusion targeted biopsies for the diagnosis of clinically significant prostate cancer. Eur Urol Oncol 2019;2(3):329–332.
19. Ghai S, Van der Kwast T. Suspicious findings on micro-ultrasound imaging and early detection of prostate cancer. Urol Case Rep 2017;16:98–100.
20. Claros OR, Tourinho-Barbosa RR, Fregeville A, et al. Comparison of initial experience with transrectal magnetic resonance imaging cognitive guided micro-ultrasound biopsies versus established transperineal robotic ultrasound magnetic resonance imaging fusion biopsies for prostate cancer. J Urol 2020;203(5):918–925.
21. Wiemer L, Hollenbach M, Heckmann R, et al. Evolution of targeted prostate biopsy by adding micro-ultrasound to the magnetic resonance imaging pathway. Eur Urol Focus 2021;7(6):1292–1299.
22. Sountoulides P, Pyrgidis N, Polyzos SA, et al. Micro-ultrasound-guided vs multiparametric magnetic resonance imaging-targeted biopsy in the detection of prostate cancer: a systematic review and meta-analysis. J Urol 2021;205(5):1254–1262.
23. Rodríguez Socarrás ME, Gomez Rivas J, Cuadros Rivera V, et al. Prostate mapping for cancer diagnosis: the Madrid Protocol. Transperineal prostate biopsies using multiparametric magnetic resonance imaging fusion and micro-ultrasound guided biopsies. J Urol 2020;204(4):726–733.
24. Eure G, Fanney D, Lin J, Wodlinger B, Ghai S. Comparison of conventional transrectal ultrasound, magnetic resonance imaging, and micro-ultrasound for visualizing prostate cancer in an active surveillance population: A feasibility study. Can Urol Assoc J 2019;13(3):E70–E77.
25. Langer DL, van der Kwast TH, Evans AJ, et al. Intermixed normal tissue within prostate cancer: effect on MR imaging measurements of apparent diffusion coefficient and T2—sparse versus dense cancers. Radiology 2008;249(3):900–908.
26. Prendeville S, Gertner M, Maganti M, et al. Role of magnetic resonance imaging targeted biopsy in detection of prostate cancer harboring adverse pathological features of intraductal carcinoma and invasive cribriform carcinoma. J Urol 2018;200(1):104–113.
27. Truong M, Feng C, Hollenberg G, et al. A comprehensive analysis of cribriform morphology on magnetic resonance imaging/ultrasound fusion biopsy correlated with radical prostatectomy specimens. J Urol 2018;199(1):106–113 [Published correction appears in J Urol 2018;199(2):576.].
28. Norris JM, Carmona Echeverria LM, Simpson BS, et al. Conspicuity of cribriform prostate cancer on multiparametric magnetic resonance imaging: the jury is still out. BJU Int 2021;127(2):169–170.
29. Villers A, Marliere F, Ouzzane A, Puech P, Lemaître L. MRI in addition to or as a substitute for prostate biopsy: the clinician's point of view. Diagn Interv Imaging 2012;93(4):262–267.
30. Stabile A, Giganti F, Emberton M, Moore CM. MRI in prostate cancer diagnosis: do we need to add standard sampling? A review of the last 5 years. Prostate Cancer Prostatic Dis 2018;21(4):473–487.
31. Ukimura O, Marien A, Palmer S, et al. Trans-rectal ultrasound visibility of prostate lesions identified by magnetic resonance imaging increases accuracy of image-fusion targeted biopsies. World J Urol 2015;33(11):1669–1676.
32. van de Ven WJ, Sedelaar JP, van der Leest MM, et al. Visibility of prostate cancer on transrectal ultrasound during fusion with multiparametric magnetic resonance imaging for biopsy. Clin Imaging 2016;40(4):745–750.
33. Cornud F, Lefevre A, Flam T, et al. MRI-directed high-frequency (29MhZ) TRUS-guided biopsies: initial results of a single-center study. Eur Radiol 2020;30(9):4838–4846.